DOI: 10.31276/VJSTE.65(3).14-20

Green synthesis of silver nanoparticles using *Mentha crispa* L. leaf extract for treatment of dye wastewater

Thi Minh Dinh[1], Khac Khoi Tran[2, 3], Anh Trung Le[2], Thi Minh Nguyet Nguyen[2], Thi Hue Do[2*], Ian Liau[4]

[1]Dai Tu High School, Hung Son Town, Dai Tu District, Thai Nguyen Province, Vietnam
[2]Faculty of Physics, Thai Nguyen University of Education, 20 Luong Ngoc Quyen Street, Quang Trung Ward, Thai Nguyen City, Thai Nguyen Province, Vietnam
[3]Faculty of Fundamental Science, Phenikaa University, Nguyen Van Trac Street, Yen Nghia Ward, Ha Dong District, Hanoi, Vietnam
[4]Department of Applied Chemistry, National Yang-Ming Chiao-Tung University, 1001, University Road, Hsinchu 300, Taiwan

Received 25 October 2022; revised 29 December 2022; accepted 5 January 2023

Abstract:

***Mentha crispa* L. is one of Vietnam's most precious folk medicines and is also a spice used in many delicious dishes in Vietnam and around the world. The use of *Mentha crispa* L. leaf extract as a reducing agent for Ag^+ ions to synthesize silver nanoparticles is discussed in this paper. Single silver nanospheres were dispersed in biological media and their sizes were controlled in the range of 20-80 nm. Factors affecting particle size and shape such as extract concentration, $AgNO_3$ concentration, reaction time, and temperature were investigated to determine the optimal parameters for particle synthesis. The optical properties, dispersion, crystal structure, morphology, and sizes of silver nanoparticles were investigated through UV-Vis absorption spectroscopy, dynamic light scattering (DLS) measurements, X-ray diffraction, and transmission electron microscopy (TEM). The functional groups on the L.AgNPs were determined by Fourier-transform infrared (FTIR) transmittance spectra. The synthesised silver nanoparticles were used to treat methylene blue (MB) dye, the main component of dye wastewater, based on their photocatalytic properties. The results show that in the presence of L.AgNPs, the photodegradation efficiency of $NaBH_4$ or H_2O_2 reducing agents is much higher, up to 95% of illumination.**

Keywords: **dyeing wastewater, green synthesis, *Mentha crispa* L., silver nanoparticles, sweet basil.**

Classification number: **2.2**

1. Introduction

Nanotechnology has been asserting its importance in many areas of science and life in almost every country in the world. Undeniably, nanomaterials are present in many products of science and technology. Silver nanoparticles are particularly interesting to scientists because of their unique properties such as their plasmon resonance frequency being located in the visible light region, non-toxicity, and high biocompatibility [1-3]. They are widely exploited in fields ranging from medicine and pharmacy, to agriculture and forestry, and to diagnostic imaging with applications such as drug delivery, cellular imaging, sensors, biological probes, and surface-enhanced Raman scattering (SERS) [4-9]. In particular, silver nanoparticles exhibit some of the best antibacterial and bactericidal activities thanks to their characteristic mechanisms [10-16]. While the antibacterial mechanism of silver nanoparticles remains controversial, observations have shown silver ions destroying respiratory function, the function of cell walls, as well as binding to the DNA of microbial cells and destroying their function [17-22]. In addition, silver nanoparticles have been shown to have redox properties that catalyse biological agents such as dyes and chemical agents like benzene under the influence of light [23-27].

Because of the wide applicability of silver nanoparticles, they have been synthesized by many different methods such as chemical reduction, electrochemistry, radiation, photochemistry, and biological reduction [28-32]. Each method creates nanoparticles with different shapes, structures, and sizes. Depending on the intended use and specific conditions, different methods are selected. Recently, synthesizing silver nanoparticles by using reducing agents of biological origin such as microorganisms and plant extracts has attracted much attention from researchers [33-36]. This method synthesizes particles with high concentration, relatively uniform size, and, especially, with abundant raw materials, low economical cost, and environmentally friendly products. The synthesis of silver nanoparticles from plant extracts has advantages over synthesis from biological microorganisms because it eliminates the elaborate process of cell culture and simplifies large-scale particle synthesis thereby saving time and cost [34-36]. There are many types of plants selected for the synthesis of silver nanoparticles such as Azadirachta indica [37], green tea leaves [38], *Aloe vera* [39], *Capsicum annuum* L. [40], *Jatropha curcas* [41], *Magnolia kobus* [42], *Carica papaya* [43], *Hibiscus rosa* Sinensis [44], *Mentha piperita* [45], *Morinda citrifolia* [46], *Sesbania grandiflora* [47], *Albizia adianthifolia* [48], and *Ziziphora tenuior* [49]. However, there have been no reports on the use of *Mentha crispa* L. leaf extract to synthesize silver nanoparticles.

Sweet basil (*Mentha crispa* L.) is a common herb in Europe, northwest Africa, and Asia. This vegetable belongs to *Mentha*

*Corresponding author: Email: huedt@tnue.edu.vn

aquatica, which is relatively similar in appearance to mint (*Mentha arvensis* L.). Many people often confuse these two herbs with each other. However, in fact, sweet basil and mint are two different vegetables. Not only is it used as a spice, sweet basil can also be used as a medicine with many effects on human health. Sweet basil can strengthen the digestive system, prevent cancer, help brighten skin, protect skin from acne, effectively fight inflammation, treat insect bites, treat sore throats, relieve colds, and treat asthma from colds [50]. In this paper, we synthesize silver nanoparticles using *Mentha crispa* L. leaf extract and study the application of these synthesized silver nanoparticles in the treatment of dye wastewater and antibacterial activity.

2. Materials and methods

2.1. Materials

Silver nitrate ($AgNO_3$, >99%) and methylene blue dye ($C_{16}H_{18}ClN_3S$, 97%) were purchased from Sigma Aldrich. Sodium borohydride ($NaBH_4$, >99%) and hydrogen peroxide (H_2O_2, 30%) were purchased from Merck, Germany. Chemicals were used without any purification. Sweet basil leaves were collected from the medicinal garden at Thai Nguyen University of Education. Deionized water (DI) with a resistance of 18.2 MΩ was used in all processes.

2.2. Mentha crispa L. leaf extract preparation

The sweet basil leaves were collected and washed several times with water and then deionized water to remove dirt adhered to the leaves. They were dried at room temperature (27^0C) for 24 hours and then ground into a powder with an agate mortar. Then, 10 g of leaf powder was mixed with 100 ml of sterilised, deionized water. The mixture was steamed in a water bath at 100°C for about 30 min. The solution was cooled and centrifuged at 5000 rpm for about 15 min. The residue was removed and the solution extract was filtered with Whatman No. 1 filter paper. The final extract was obtained by filtering the solution through a 0.22-µm Ministart filter and was stored refrigerated (4°C) for future use.

2.3. Green synthesis of silver nanoparticles (L.AgNPs)

An amount of *Mentha crispa* L. leaf extract in respective volumes was mixed into a 1.0 mM $AgNO_3$ solution. The reaction mixture was continuously magnetically stirred in the dark at room temperature for about 24 hours. The reactions of the solution were monitored at different time intervals. To optimize the synthesis of L.AgNPs, the influences of $AgNO_3$ concentration, reaction time, and extract volume were investigated. The volumes of $AgNO_3$ in the series of experiments to investigate the effect of $AgNO_3$ concentration were 6, 8, 10 and 14 ml, respectively, corresponding to $AgNO_3$ concentrations varying from 0.43 to 0.8 mM while the volume of extract solution was 0.25 ml. To investigate the effect of the amount of extract on the particle synthesis yield, different volumes of extract were used: 0.15, 0.25 and 0.35 ml while the volume of 1 mM $AgNO_3$ solution was 14 ml. At the same time, to monitor the development of L.AgNPs over time, each solution was withdrawn from the reaction vessel at certain times such as 0.5, 2, 4, 6, 8,10, 12, 14, 16 and 24 hours. The synthesis process of the L.AgNPs is shown in Fig. 1.

2.4. Application of L.AgNPs

L.AgNPs were used as photocatalysts to treat MB, an ingredient in dye wastewater in either 30% H_2O_2 or 0.2 M $NaBH_4$. To examine the role of L.AgNPs in improving the degradation efficiency of MB pigment, experiments were conducted independently in the presence or absence of L.AgNPs as a catalyst. Specifically, 10 ml of L.AgNP solution, after centrifugation to remove impurities, was placed into 100 ml of 10-ppm MB solution and magnetically stirred in the dark for about 2 hours to balance absorption. Then, 1 ml of 30% H_2O_2 or 2 ml of 0.2 M $NaBH_4$ were added to the solution. The mixture was continuously illuminated with a 30 W LED with a colour temperature of 6500 K (Philips, Amsterdam, The Netherlands). The photodegradation rate was monitored by observing the absorption reduction at the characteristic peak of MB pigment after each illumination time period: 5, 30, 60, 90, and 120 min.

2.5. Characterisation

A Jasco V-770 UV-Vis spectrophotometer was used to investigate the optical properties of the synthesised silver nanoparticles at wavelengths between 250-1000 nm. Morphology and particle size were determined by TEM on a JEOL JEM-2100 at an accelerating voltage of 200 kV. The particle size distribution of the L.AgNPs in media was evaluated by a particle size analyser (PSA, Delta Nano C, Beckman) using DLS. The XRD spectra were collected using an X-ray diffractometer (Bruker D8 Advance, Germany) operated at 30 kV with Cu-K_α radiation (wavelength of λ=0.154056 nm) with a parallel-beam geometry between 30 to 80°. The main functional groups of the *Mentha crispa* L. leaf extract and L.AgNPs were analysed by FTIR spectra using an FTIR spectrophotometer (Nicolet 6700, Thermo Scientific) (Fig. 1).

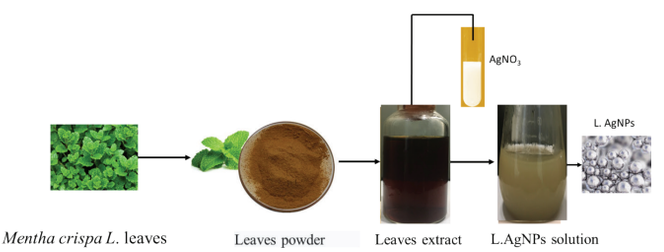

Fig. 1. Process for synthesising L.AgNPs from *Mentha crispa* L. leaf extract.

3. Results and discussion

The influence of $AgNO_3$ concentration, amount of extract, and reaction time on the morphology and size of the L.AgNPs is shown through the absorption spectrum of the solutions (Fig. 2). Figs. 2A and 2B are the absorption spectra and the normalised absorption spectra of the L.AgNPs solutions when the $AgNO_3$ concentration was varied from 0.43 to 0.8 mM. It can be seen that $AgNO_3$ concentration has a great influence on the formation and growth of particles as both the absorbance and resonance peak

wavelengths change with $AgNO_3$ concentration. When the $AgNO_3$ concentration is below 0.75 mM, the produced L.AgNPs are not uniform in size. This is shown by the half-width of the normalised absorption spectra. When $AgNO_3$ concentration is 0.8 mM, the half-spectral width is much narrower, and the absorption spectrum at its lowest. It was demonstrated that the synthesised L.AgNPs have a relatively uniform size of around 40 nm (corresponding to the absorption peak at 445 nm). The effect of $AgNO_3$ concentration on particle formation and growth was explained by a kinetic mechanism according to Lamer's model [51]. When the $AgNO_3$ concentration is high, the reaction rate is fast during the first stage and the concentration of monomers rapidly increases, facilitating the formation of small-size particles and relatively uniform size development in the later stages.

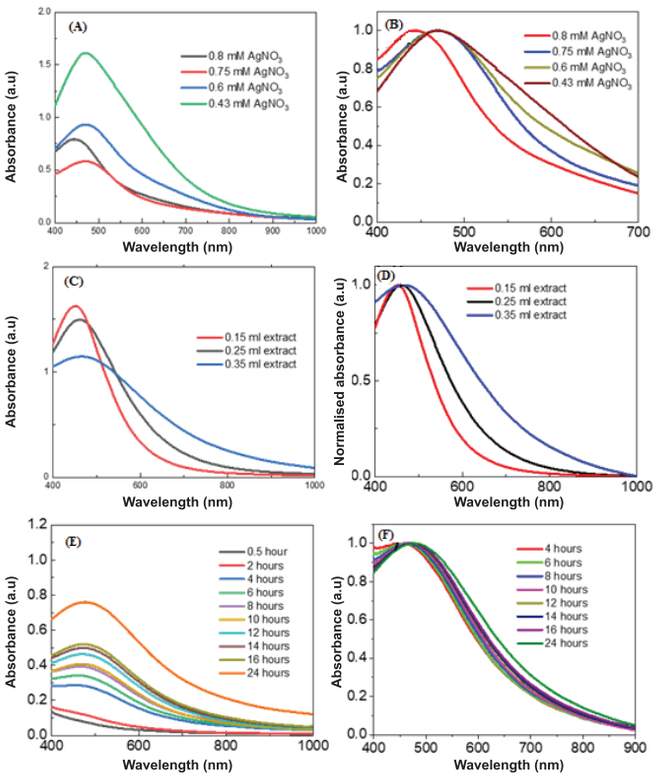

Fig. 2. The dependence of UV-VIS and normalised absorption spectra of L.AgNP solutions on $AgNO_3$ concentration (A, B), extract volume (C, D), and reaction time (E, F).

Extraction volume also greatly influenced the formation and growth of the L.AgNPs (Figs. 2C and 2D). With extraction volumes of 0.25 and 0.35 ml, the absorbance spectra showed a large amount of excess extract after the reaction as shown by the high absorbance in the region below 400 nm. At the same time, L.AgNPs formed in different sizes, especially when the extract volume was 0.35 ml. Thus, in this survey, an extract volume of 0.15 ml synthesised the best quality L.AgNPs. The extract acts as a reducing agent in particle fusion. In these reactions, the volume of extract used was in excess of the amount of precursor $AgNO_3$, so it can be seen that the larger the extract volume, the more inhibited the incorporation of monomers in solution during the early stages of the reaction. This leads to heterogeneous formation of particles in the solution and a larger size distribution. On the other hand, as the kinetic processes behind the formation and growth of particles go through each stage, time plays an important role in the synthesis reaction. In this study, the volume of extract used was 0.5 ml and the volume of 1 mM $AgNO_3$ was 20 ml. After a certain period of time, 2 ml of the solution was withdrawn to investigate the optical characteristics, morphology, and size. In the first 4 hours of the reaction, the L.AgNPs in solution began to form but with low concentration and small size corresponding to an absorption spectrum that had no clear resonance peak (characteristic spectrum of metal nanoparticles as small as 10 nm in diameter) [52]. As the reaction time increased, the absorbance increased and the resonance peak shifted towards longer wavelengths, indicating more particles were formed and the size increased. However, in the absorption spectrum at 24 hours, it can be seen that the half-width of the peak tended to increase and large particles formed as evidenced by the increased absorption at longer wavelengths. The formation and growth of AgNPs over time are also explained by the Lamer mechanism [51]. However, the initial phase of this kinetic process is long because the reduction reaction rate is slow. When the reaction time lasts more than 24 hours, to the point where no new monomers are generated, particles will agglomerate together to form larger particles in the solution.

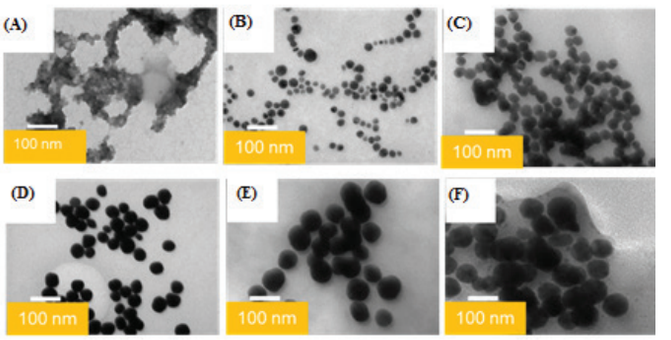

Fig. 3. TEM image of L.AgNPs by reaction time. (A) 4 hours, **(B)** 6 hours, **(C)** 10 hours, **(D)** 14 hours, **(E)** 16 hours, **(F)** 24 hours.

This process is shown by observing the TEM images of the particles obtained at different time intervals (Fig. 3). A reaction time of fewer than 2 hours yielded hardly any L.AgNPs. An appearance of beads in the TEM measurement was obtained when the reaction time was over 4 hours. However, after 4 hours of reaction, mainly small particles (several nm) were formed and tended to clump together. When reaction time increased from 6 to 24 hours, the average size of the L.AgNPs particles increased from 20 to 80 nm. Fig. 3F shows 24 hours of reaction time and the obtained particles are of unequal size, agglomerating to form large-sized particles, and at the same time very small particles appear. From this data, it seems that a synthesis time of 16 hours for L.AgNPs from the extract of basil leaves is the most suitable (Fig. 3E). These results prove that using organic compounds to reduce Ag^+ ions is much faster than using fungi or bacteria to synthesise silver particles [53].

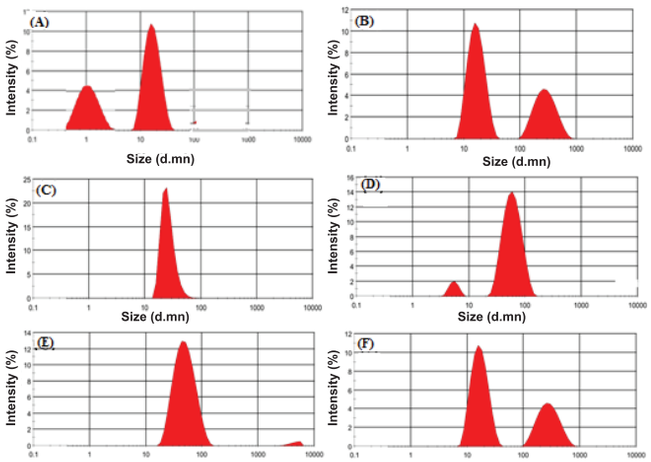

Fig. 4. Dependence of particle size distribution spectra of L.AgNPs on reaction time. (A) 2 hours, **(B)** 6 hours, **(C)** 10 hours, **(D)** 14 hours, **(E)** 16 hours, **(F)** 24 hours.

Fig. 4 shows the particle size distribution spectra of the L.AgNPs obtained after different reaction times. It can be seen that silver nanoparticles synthesised from plant extracts have a wider size distribution than silver nanoparticles synthesised by chemical reduction because of slower biological reduction reactions. Even so, the results obtained show that synthesis efficiency as well as the particle size uniformity are better than those previously published using green synthesis methods [33-35]. The XRD spectra of the L.AgNPs synthesised at 10, 14, 16, and 24 hours are shown in Fig. 5. It can be seen that the samples all have the same peaks at 2θ angles 27.8, 32.2, 38.1, 43.6, 46.4, 64.4, and 77.5° corresponding to the lattice planes (211), (122), (111), (200), (231), (220), and (311), respectively, of face-centred cubic (fcc) Ag crystals [52]. No peaks from any other phase appeared in the XRD spectrum, indicating that a single phase of Ag with cubic structure nanoparticles was synthesised directly from the extract. The average crystal size was determined based on the width of the diffraction peaks using the Debye-Scherrer formula: $D=(k\lambda)/(\beta \cos \theta)$, where D is the average crystal size of the powder sample; K=0.9 is the geometric factor or Scherrer constant; β is the angular full-width at half maximum (FWHM) of the XRD peak (rad), λ=0.154056 nm is the wavelength of Cuk_{α}, and θ is the Bragg diffraction angle of the corresponding peak. For the samples surveyed, the diffraction peak with the highest intensity occurred at 2θ=38.1°, corresponding to the (111) lattice plane. The average crystal size determined according to this diffraction peak is 0.44 nm.

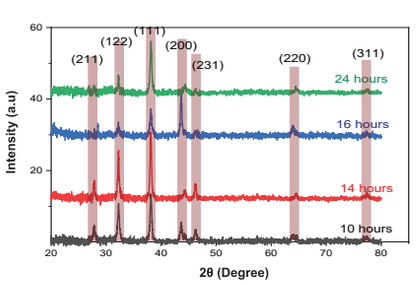

Fig. 5. XRD spectrum of the L.AgNPs at different reaction times.

The FTIR spectra of the L.AgNPs showed the presence of functional groups on the particles in the wavenumber range from 540 to 3444 cm^{-1} (Fig. 6). The region of greatest intensity at 3444 cm^{-1} is attributed to the presence of -OH functional groups of alcohol and phenolic compounds, which exist in the basil leaf extract [44, 45]. Peaks in the region of 1631 to 1387 cm^{-1} are attributed to the stretching vibrations of the C-N bonds of amide functional groups.

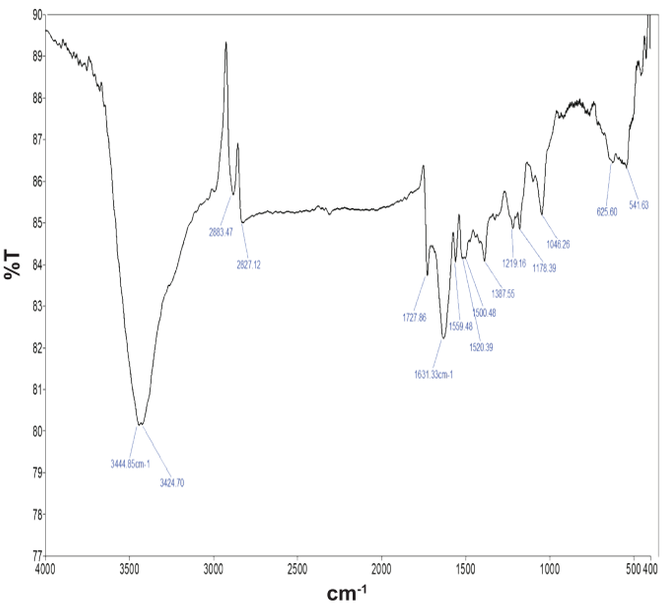

Fig. 6. FTIR spectrum of L.AgNPs.

Peaks in the 1178 and 1220 cm^{-1} regions are attributed to the C-N stretching mode of aromatic amine groups. The peak at 1048 cm^{-1} is related to the presence of C-O bonds. The band at 1048 cm^{-1} is also related to the presence of C-O bonds. The peaks in the 541 to 625 cm^{-1} region represent fluctuations of metallic Ag [47, 48].

L.AgNPs were used as a catalyst to study the ability to degrade MB organic pigment in the presence of either H_2O_2 or $NaBH_4$ reducing agents. The experiments were conducted under the condition that the solution was illuminated with a 30 W LED white light source of colour temperature 6500 K. The illumination was carried out continuously for 2 hours to monitor the photodegradation efficiency of the L.AgNPs. Fig. 7 shows the absorption spectra of the 10 ppm MB solution over the illumination time in the cases of using only 0.2 M $NaBH_4$ (Fig. 7A), only L.AgNPs (Fig. 7B), only 30% H_2O_2 (Fig. 7C), 30% H_2O_2 reducing agent catalysed by L.AgNPs (Fig. 7D), and 0.2 M $NaBH_4$ reducing agent catalysed by L.AgNPs (Fig. 7E). In the spectroscopic determination of the decrease in relative absorbance of MB pigment in the cases over time of illumination (Fig. 7F), the colour of the solution changed with the exposure time when using H_2O_2 reducing agent (Fig. 7G) and $NaBH_4$ reducing agent (Fig. 7H) with the catalyst L.AgNPs. Monitoring the decrease of

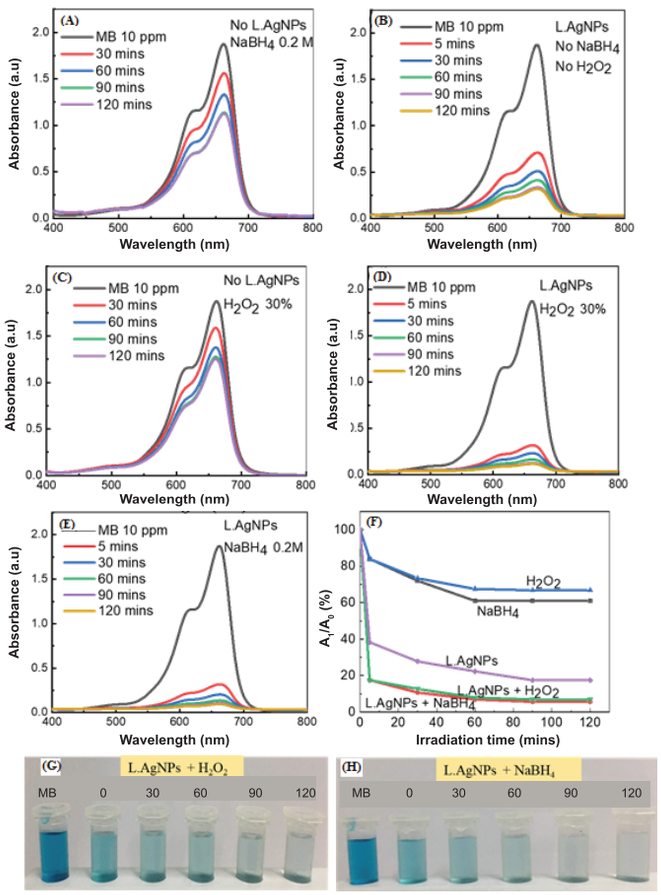

Fig. 7. Absorption spectrum of MB over time in the following cases: (A) only $NaBH_4$, (B) only L.AgNPs, (C) only H_2O_2, (D) L.AgNPs + H_2O_2, (E) L.AgNPs + $NaBH_4$, (F) the decrease in relative absorbance of MB with time, (G, H) changes to the colour of the solutions with time.

absorbance of MB at 662 nm with irradiation time, it can be seen that when the reducing agents H_2O_2 or $NaBH_4$ and L.AgNPs are not used simultaneously, an absorbance of MB at the solid peak is observed. The 662 nm peak also decreased when illuminated. However, the absorbance can only be reduced to a certain value and cannot be further reduced. This shows that under the effect of light and reducing agents, MB is also partially discoloured (Figs. 7A and 7C). In the case where the MB colorant solution contains only L.AgNPs and is illuminated, the photodegradability is better than that of the solutions without L.AgNPs. In 2 hours, the absorbance of MB decreased from 1.87 to 0.34 when catalysed by L.AgNPs. This clearly demonstrates the role of Ag nanoparticles in the degradation of MB pigment. To demonstrate this, experiments monitoring the photodegradability of Ag nanosheets were performed using both reducing agents and L.AgNPs (Figs. 7D and 7E). The results showed that after irradiation for about 1 hour, the absorption concentration of MB in the solution decreased significantly, and after 2 hours of illumination, almost all the pigments were decomposed. This can be seen by the colour of the solutions over time (Figs. 7G and 7H). There is a slight difference between using H_2O_2 and $NaBH_4$ reducing agents in terms of photodegradation efficiency (Fig. 7F). The photodegradation efficiency is better when using $NaBH_4$, although the concentration of $NaBH_4$ reducing agent is much lower than that of H_2O_2. The photodegradation efficiency was determined by the following formula:

$$H = \frac{A_0 - A_t}{A_0} \times 100\%$$

where A_o is the absorbance of the initial MB and A_t is the absorbance of the MB at the peak of 662 nm after the illumination time t. Therefore, from the data on the absorption spectrum, it can be determined that the photodegradation efficiency in the case of L.AgNPs and 30% H_2O_2 is 92.6% and in the case of 0.2 M L.AgNPs and $NaBH_4$ it is 95.6%. The photodegradation mechanism of the L.AgNPs is explained by the light absorption of silver nanoparticles along with the presence of NaBH4 reducing agent, making the colour degradation reaction speed faster.

$AgNPs + h\nu \rightarrow Ag^+ (e^-, h^+)$

$h^+ + MB + NaBH_4 \rightarrow$ colourless products

4. Conclusions

In this article, spherical L.AgNPs with sizes ranging from 20 to 80 nm in diameter were synthesised by a simple de-greening method using basil leaf extract. The size, as well as the particle size distribution, depended on the extract volume, $AgNO_3$ concentration, and reaction time. The survey results of factors affecting the formation and growth of L.AgNPs showed that when the concentration of $AgNO_3$ was 0.8 mM and the extraction volume was 0.15 ml, the L.AgNPs had an average size of 40 nm and the particles were relatively uniform in shape and size. The synthesis time of the L.AgNPs by the extraction method is about 6 hours, which is much shorter than the synthesis time using bacteria or fungi. Increasing synthesis time from 6 to 24 hours caused the average size of the L.AgNPs to increase from 20 to 80 nm. However, the most reasonable time to obtain L.AgNPs with the best quality was between 10 and 16 hours. The L.AgNPs were used to study photocatalytic ability of colour degradation of MB. Comparing the results of MB's absorbance attenuation at the 662 nm peak in cases with and without L.AgNPs, it was seen that the L.AgNPs have an important role in photodegradation. The highest photodegradation efficiency was 95% when using 0.2 M $NaBH_4$ reducing agent together with the Ag catalyst.

CRediT author statement

Thi Minh Dinh: Methodology, Formal analysis, Writing, Editing; Khac Khoi Tran: Material synthesis, Data analysis, Editing; Anh Trung Le: Material synthesis, Writing, Review;

Thi Minh Nguyet Nguyen: Review, Data analysis; Thi Hue Do: Material synthesis, Data analyst, Review, Writing, Editing; Ian Liau: Editing, Data analyst.

ACKNOWLEDGEMENTS

The present research was supported by Vietnam Ministry of Education and Training under grant code B2023-TNA-06.

COMPETING INTERESTS

The authors declare that there is no conflict of interest regarding the publication of this article.

REFERENCES

[1] M. Asif, R. Yasmin, S. Umbreen (2022), "Green synthesis of silver nanoparticles (agnps), structural characterization, and their antibacterial potential", *Dose-Response*, **20(2)**, DOI: 10.1177/15593258221088709.

[2] C. Liao, Y. Li, S.C. Tjong (2019), "Bactericidal and cytotoxic properties of silver nanoparticles", *International Journal of Molecular Sciences*, **20(2)**, pp.449-452, DOI: 10.3390/ijms20020449.

[3] E.Y. Ahn, H. Jin, Y. Park (2019), "Assessing the antioxidant, cytotoxic, apoptotic and wound healing properties of silver nanoparticles green-synthesized by plant extracts", *Materials Science and Engineering C*, **101**, pp.204-216, DOI: 10.1016/j.msec.2019.03.095.

[4] R.A. Bapat, T.V. Chaubal, C.P. Joshi, et al. (2018), "An overview of application of silver nanoparticles for biomaterials in dentistry", *Materials Science and Engineering C*, **91**, pp.881-898, DOI: 10.1016/j.msec.2018.05.069.

[5] S. Nakamura, M. Sato, Y. Sato, et al. (2019), "Synthesis and application of silver nanoparticles (ag nps) for the prevention of infection in healthcare workers", *International Journal of Molecular Sciences*, **20(15)**, DOI: 10.3390/ijms20153620.

[6] K. Chand, D. Cao, D.E. Fouad, et al. (2020), "Green synthesis, characterization and photocatalytic application of silver nanoparticles synthesized by various plant extracts", *Arabian Journal of Chemistry*, **21(11)**, pp.8248-8261, DOI: 10.1016/j.arabjc.2020.01.009.

[7] A. Akbarzadeh, L. Kafshdooz, Z. Razban, et al. (2018), "An overview application of silver nanoparticles in inhibition of herpes simplex virus", *Artificial Cells, Nanomedicine, and Biotechnology*, **46(2)**, pp.263-267, DOI: 10.1080/21691401.2017.1307208.

[8] K. Zhang, V.C.H. Lui, Y. Chen, et al. (2020), "Delayed application of silver nanoparticles reveals the role of early inflammation in burn wound healing", *Scientific Reports*, **10(1)**, DOI: 10.1038/s41598-020-63464-z.

[9] S. Lee, B.H. Jun (2019), "Silver nanoparticles: synthesis and application for nanomedicine", *International Journal of Molecular Sciences*, **20(4)**, DOI: 10.3390/ijms20040865.

[10] A.S. Anees, S.S. Das, A. Khatoon, et al. (2020), "Bactericidal activity of silver nanoparticles: A mechanistic review", *Materials Science for Energy Technologies*, **3(1)**, pp.756-769, DOI: 10.1016/j.mset.2020.09.002.

[11] S.K. Kailasa, T.J. Park, J.V. Rohit, J.R. Koduru (2019), "Antimicrobial activity of silver nanoparticles", *Nanoparticles in Pharmacotherapy*, **2019**, pp.461-484, DOI: 10.1016/b978-0-12-816504-1.00009-0.

[12] A. Roy, O. Bulut, S. Some (2019), "Green synthesis of silver nanoparticles: biomolecule-nanoparticle organizations targeting antimicrobial activity', *RSC Advances*, **9(5)**, pp.2673-2702, DOI: 10.1039/c8ra08982e.

[13] J.Y. Cheon, S.J. Kim, Y.H. Rhee, et al. (2019), "Shape-dependent antimicrobial activities of silver nanoparticles", *International Journal of Nanomedicine*, **14**, pp.2773-2780, DOI: 10.2147/IJN.S196472.

[14] C.G. Anjali Das, V.G. Kumar, T.S. Dhas, et al. (2020), "Antibacterial activity of silver nanoparticles (biosynthesis): A short review on recent advances", *Biocatalysis and Agricultural Biotechnology*, **27**, DOI: 10.1016/j.bcab.2020.101593.

[15] M.G. Gordienko, V.V. Palchikova, S.V. Kalenov, et al. (2019), "Antimicrobial activity of silver salt and silver nanoparticles in different forms against microorganisms of different taxonomic groups", *Journal of Hazardous Materials*, **378**, DOI: 10.1016/j.jhazmat.2019.120754.

[16] T. Bruma, F. Maldonado-Bravo, P. Jara, et al. (2021), "Silver nanoparticles and their antibacterial applications", *International Journal of Molecular Sciences*, **22(13)**, DOI: 10.3390/ijms22137202.

[17] X. Yan, B. He, L. Liu, et al. (2018), "Antibacterial mechanism of silver nanoparticles in pseudomonas aeruginosa: Proteomics approach", *Metallomics*, **10(4)**, pp.557-564, DOI: 10.1039/C7MT00328E.

[18] Y. Qing, L. Cheng, R. Li, et al. (2018), "Potential antibacterial mechanism of silver nanoparticles and the optimization of orthopedic implants by advanced modification technologies", *International Journal of Nanomedicine*, **13**, pp.3311-3327, DOI: 10.2147/ijn.s165125.

[19] S. Tang, J. Zheng (2018), "Antibacterial activity of silver nanoparticles: Structural effects", *Advanced Healthcare Materials*, **7(13)**, DOI: 10.1002/adhm.201701503.

[20] S. Liao, Y. Zhang, X. Pan, et al. (2019), "Antibacterial activity and mechanism of silver nanoparticles against multidrug-resistant Pseudomonas aeruginosa", *Int. J. Nanomedicine*, **25(14)**, pp.1469-1487, DOI: 10.2147/IJN.S191340.

[21] G. Navarro, E. Alpaslan, M. Wang, et al. (2019), "Characterization and study of the antibacterial mechanisms of silver nanoparticles prepared with microalgal exopolysaccharides", *Materials Science and Engineering C*, **99**, pp.685-695, DOI: 10.1016/j.msec.2019.01.134.

[22] A. Salleh, R. Naomi, N.D. Utami, et al. (2020), "The potential of silver nanoparticles for antiviral and antibacterial applications: A mechanism of action", *Nanomaterials*, **10(8)**, pp.1566-1572, DOI: 10.3390/nano10081566.

[23] R. Rajkumar, G. Ezhumalai, M. Gnanadesigan (2020), "A green approach for the synthesis of silver nanoparticles by *Chlorella vulgaris* and its application in photocatalytic dye degradation activity", *Environmental Technology & Innovation*, **21**, DOI: 10.1016/j.eti.2020.101282.

[24] M.A. Kareem, I.T. Bello, H.A. Shittu, et al. (2020), "Green synthesis of silver nanoparticles (AgNPs) for optical and photocatalytic applications: A review", *IOP Conference Series: Materials Science and Engineering*, **805**, DOI: 10.1088/1757-899X/805/1/012020.

[25] J. Singh, S.S. Jolly, K.H. Kim, et al. (2019), "Biogenic synthesis of silver nanoparticles and its photocatalytic applications for removal of organic pollutants in water", *Journal of Industrial and Engineering Chemistry*, **80(1)**, pp.247-257, DOI: 10.1016/j.jiec.2019.08.002.

[26] G.B. Strapasson, A.G. Kontos (2021), "Microwave assisted synthesis of silver nanoparticles and its application in sustainable photocatalytic hydrogen evolution", *International Journal of Hydrogen Energy*, **46(69)**, pp.34264-34275, DOI: 10.1016/j.ijhydene.2021.07.23.

[27] M.S. Samuel, S. Jose, E. Selvarajan, et al. (2019), "Biosynthesized silver nanoparticles using Bacillus amyloliquefaciens; Application for cytotoxicity effect on A549 cell line and photocatalytic degradation of p-nitrophenol", *Journal of Photochemistry and Photobiology B*, **202**, DOI: 10.1016/j.jphotobiol.2019.111642.

[28] K. Gudikandula, S. Charya Maringanti (2016), "Synthesis of silver nanoparticles by chemical and biological methods and their antimicrobial properties", *Journal of Experimental Nanoscience*, **11(9)**, pp.1-8, DOI: 10.1080/17458080.2016.1139196.

[29] M. Rafique, I. Sadaf, M.S. Rafique, et al. (2016), "A review on green synthesis of silver nanoparticles and their applications", *Artificial Cells Nanomedicine, and Biotechnology*, **45(7)**, pp.1-20, DOI: 10.1080/21691401.2016.1241792.

[30] D.T. Hue, N.T.P. Thao, T.K. Khoi, et al. (2021), "Multi-shaped silver meso-particles with tunable morphology for surface enhanced Raman scattering", *Optics Communications*, **497**, DOI: 10.1016/j.optcom.2021.127200.

[31] A. Ahmed, M. Ahmad, B.L. Swami, et al. (2015), "A review on plants extract mediated synthesis of silver nanoparticles for antimicrobial applications: A green expertise", *Journal of Advanced Research*, **7(1)**, pp.17-28, DOI: 10.1016/j.jare.2015.02.007.

[32] R. Shanmuganathan, I. Karuppusamy, M. Saravanan, et al. (2019), "Synthesis of silver nanoparticles and their biomedical applications - A comprehensive review", *Current Pharmaceutical Design*, **25(24)**, pp.2650-2660, DOI: 10.2174/1381612825666190708185506.

[33] M. Ahmed, G. Murtaza, A. Mehmood, et al. (2015), "Green synthesis of silver nanoparticles using leaves extract of Skimmia laureola: Characterization and antibacterial activity", *Materials Letters*, **153**, pp.10-13, DOI: 10.1016/j.matlet.2015.03.143.

[34] S. Kumar, B. Ankamwar, S. Karmakar, et al. (2018), "Green synthesis of silver nanoparticles using the plant extract of Shikakai and Reetha", *Materials Today: Proceedings*, **5(1)**, pp.2321-2329, DOI: 10.1016/j.matpr.2017.09.236.

[35] P. Tamilarasi, P. Meena (2020), "Green synthesis of silver nanoparticles (Ag NPs) using Gomphrena globosa (Globe amaranth) leaf extract and their characterization", *Materials Today: Proceedings*, **33(5)**, pp.2209-2216, DOI: 10.1016/j.matpr.2020.04.025.

[36] T. Varadavenkatesan, R. Selvaraj, R. Vinayagam (2019), "Green synthesis of silver nanoparticles using Thunbergia grandiflora flower extract and its catalytic action in reduction of Congo red dye", *Materials Today: Proceedings*, **23(1)**, pp.39-42, DOI: 10.1016/j.matpr.2019.05.441.

[37] N. Namratha, P.V. Monica (2013), "Synthesis of silver nanoparticles using *Azadirachta indica* (Neem) extract and usage in water purification", *Asian Journal of Pharmacy and Technology*, **3(4)**, pp.170-174.

[38] H.A. Widatalla, L.F. Yassin, A.A. Alrasheid, et al. (2022), "Green synthesis of silver nanoparticles using green tea leaf extract, characterization and evaluation of antimicrobial activity", *Nanoscale Advances*, **4(3)**, pp.911-915, DOI: 10.1039/D1NA00509J.

[39] P.J. Burange, M.G. Tawar, R.A. Bairagi, et al. (2021), "Synthesis of silver nanoparticles by using *Aloe vera* and *Thuja orientalis* leaves extract and their biological activity: A comprehensive review", *Bull. Natl. Res. Cent.*, **45**, DOI: 10.1186/s42269-021-00639-2.

[40] S. Li, A. Xie, X. Yu (2007), "Green synthesis of silver nanoparticles using Capsicum *annuum* L. extract", *Chemistry*, **9(8)**, DOI: 10.1039/b615357g.

[41] S. Nayak, S.P. Sajankila, C.V. Rao, et al. (2019), "Biogenic synthesis of silver nanoparticles using *Jatropha curcas* seed cake extract and characterization: Evaluation of its antibacterial activity", *Energy Sources, Part A: Recovery, Utilization, and Environmental Effects*, **43(24)**, pp.1-9, DOI: 10.1080/15567036.2019.1632394.

[42] H.J. Lee, J.Y. Song, B.S. Kim (2013), "Biological synthesis of copper nanoparticles usingMagnolia kobusleaf extract and their antibacterial activity", *Journal of Chemical Technology & Biotechnology*, **1**, DOI: 10.1002/jctb.4052.

[43] S.P. Singh, A. Mishra, R.K. Shyanti, et al. (2021). "Silver nanoparticles synthesized using carica papaya leaf extract ($AGNP_S$-PLE) causes cell cycle arrest and apoptosis in human prostate (du145) cancer cells", *Biol. Trace Elem. Res.*, **199**, pp.1316-1331, DOI: 10.107/s12011-020-02255-2.

[44] L. Le, M. Fan, B. Liu, et al. (2022), "Green formulation of Ag nanoparticles by Hibiscus rosa-sinensis: Introducing a navel chemotherapeutic drug for the treatment of liver cancer", *Arabian Journal of Chemistry*, **15(2)**, DOI: 10.1016/j.arabjc.2021.103602.

[45] W. Wenzhi, P. Ma, Q. Zhao, et al. (2022), "Beneficial properties of the biosynthesized silver/chitosan nanoparticles mediated by *Mentha piperita* in rats with heart failure following myocardial infarction", *Inorganic Chemistry Communications*, **141**, DOI: 10.1016/j.inoche.2022.109581.

[46] L.V. Morales, H. Espinoza-Gómez, L.Z. Flores-López, et al. (2020), "Study of the effect of the different parts of *Morinda citrifolia* L. (noni) on the green synthesis of silver nanoparticles and their antibacterial activity", *Applied Surface Science*, **537**, DOI: 10.1016/j.apsusc.2020.147855.

[47] D.N.P. Sudarmani, S.S. Saravana, C. Sundareswari, et al. (2021), "Bioefficacy of sesbania grandiflora leaves silver nanoparticles against aedes aegypti larvae", *Journal of Advanced Scientific Research*, **12(4)**, pp.176-184, DOI: 10.55218/JASR.s1202112419.

[48] M. Dadashpour, A. Firouzi-Amandi, M.P. Moghaddam, et al. (2018), "Biomimetic synthesis of silver nanoparticles using *Matricaria chamomilla* extract and their potential anticancer activity against human lung cancer cells", *Materials Science and Engineering C*, **92**, pp.902-912, DOI: 10.1016/j.msec.2018.07.053.

[49] B. Sadeghi, F. Gholamhoseinpoor (2015), "A study on the stability and green synthesis of silver nanoparticles using Ziziphora tenuior (Zt) extract at room temperature", *Spectrochimica Acta. Part A, Molecular and Biomolecular Spectroscopy*, **134**, pp.310-315, DOI: 10.1016/j.saa.2014.06.046.

[50] K. Bączek, O. Kosakowska, M. Gniewosz, et al. (2019), "Sweet basil (*Ocimum basilicum L.*) productivity and raw material quality from organic cultivation", *Agronomy*, **9(6)**, 15pp, DOI: 10.3390/agronomy9060279.

[51] E.C. Vreeland, J. Watt, G.B. Schober, et al. (2015), "Enhanced nanoparticle size control by extending LaMer's mechanism", *J. Chemistry of Materials*, **27(17)**, pp.6059-6066, DOI: 10.1021/acs.chemmater.5b02510.

[52] K.L. Kelly, E. Coronado, L.L. Zhao, et al. (2003), "The optical properties of metal nanoparticles: The influence of size, shape, and dielectric environment", *The Journal of Physical Chemistry B,* **107(3)**, pp.668-677, DOI: 10.1021/jp026731y.

[53] M. Alavi (2022), "Bacteria and fungi as major bio-sources to fabricate silver nanoparticles with antibacterial activities", *Expert Review of Anti-infective Therapy*, **20(6)**, pp.897-906, DOI: 10.1080/14787210.2022.2045194.